

Research Highlights

Dilute magnetic semiconductors and Spintronics

Spintronics is a branch of electronics emerged from the dilute magnetic semiconductor in an aspect of utilization of the spin in addition to the charge of the carrier in a semiconductor. At present the electronics industry relies on control of charge transfer over a semiconductor ignoring the spin of the electron. The manipulation of the spin of the electrons along with the charge will open up a faster and more efficient mode of information storage and transfer for quantum computation and communication. The importance of the spin of the electrons first realized after the discovery of the giant magneto resistance in 1988, which resulted high density data storage devices, MRAM. The aspiration of future electronics devices after the Moore law limit is banked on the ferromagnetic semiconductors.

A significant amount of present solid state research has been devoted in developing and understanding as well as discovering materials for Spintronics. A large portion of the present researches are devoted to the II-VI and III-V based dilute magnetic semiconductors. As far as practical application is concerned it is desired to have room temperature ferromagnetism and materials with existing technology, which is far above the present material scenario of spintronics. Based on several theoretical investigations, it has been realized that the high Curie temperature ($> 300\text{K}$) ferromagnetism in dilute magnetic system can be achieved in ZnO or GaN of binary semiconductors in the presence of sizable amount of holes and about 5 mole % of Mn.

However, the practical difficulty of retaining p-type carriers and transition metal ions without segregating or clusterizing in these materials resulted in a question to the ferromagnetism in them. The diversions of attention beyond these materials lead to the search for new host semiconducting materials in complex oxides, nitride, phosphides, selenide, telurides etc. and doping with various kind magnetic ions. Later discovery of ferromagnetism in CdGeP_2 with small concentration of Mn^{2+} ions draws attention towards ternary and binary phosphide semiconductors. Extensive reports are available on the ternary chalcopyrite type semiconductors, like ZnSiP_2 , ZnGeP_2 , CdGeP_2 and binary phosphides, like GaP, InP, AlP etc. In most of the experiments, the transition from ferromagnetic to paramagnetic phase is reported at about 300 K, which is close to the ferromagnetic to paramagnetic transition temperature for MnP. Hence, a controversy over a carrier mediated ferromagnetism or segregated MnP remained. Thus, an exploratory search for the discovery of new semiconducting lattice suitable for hosting magnetic ions remained an open challenge for us. In this aspect we have been involved in the synthesis, crystal growth of novel materials and existing materials in alternate routes, and correlating their crystal structure with properties.

Salient results from our group

Mixed phosphides in Sn-P and Sn-Mn-P systems

In Sn-P system, several binary compounds, like, Sn_4P_3 , SnP , Sn_3P_4 , SnP_3 etc. have been reported in literature. These binary compounds have been prepared from elemental Sn and P, by an optimized preparation condition. The phosphorous rich region of Sn-P system has been investigated by us. The detailed crystal structures of various compounds in this system have been verified. In addition we have determined the crystal structure of Sn_3P_4 in detail. All the three compounds crystallize in rhombohedral lattice with space group R-3m (No. 166). The observed unit cell parameters for Sn_3P_4 , Sn_4P_3 and SnP_3 are: $a = 4.4362(1)$ and $c = 28.4220(5)$ Å; $a = 3.9648(1)$ and $c = 35.3051(5)$ Å; $a = 7.3730(1)$ and $c = 10.5361(4)$ Å, respectively. The three different crystal structures differ in the arrangement of P atoms in the unit cell. Isolated phosphorous atoms and typical Sn-Sn bonding are observed in both Sn_3P_4 and Sn_4P_3 structures. Both Sn and P atoms have octahedral environment in Sn_4P_3 structure. Complex polyhedral natures of cations (with CN 8 and 10) are observed in Sn_3P_4 structure. The P atoms in SnP_3 are coordinated to Sn and P atoms and a typical isolated hexagonal ring of P atoms exist in this structure. The crystal structure of Sn_3P_4 and SnP_3 are shown in Fig. 1 and 2, respectively.

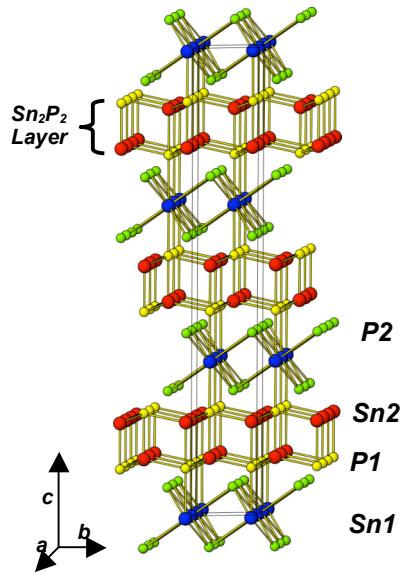


(Fig. 1)

Crystal structure of Sn_3P_4

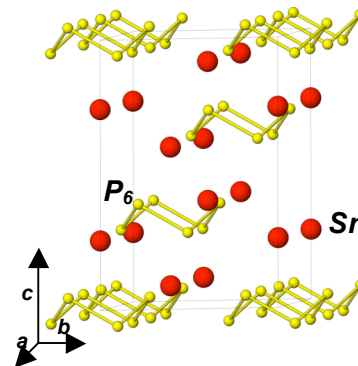


(Fig. 2)

Crystal structure of SnP_3

Mn substituted Sn_3P_4 and SnP_3 compositions like, $\text{Sn}_{3-x}\text{Mn}_x\text{P}_4$ and $\text{Sn}_{1-x}\text{Mn}_x\text{P}_3$ were prepared and studied in detail. No significant change in unit cell parameters compared to the parent host lattice is observed. The magnetizations of the samples were recorded in the temperature range of 370 to 5 K using a SQUID magnetometer (Fig.3 and 4). The magnetic behavior of the samples shows a paramagnetic to ferromagnetic

transition around 312 K, in addition to a ferromagnetic to antiferromagnetic transition around 50 K, quite similar to the features of MnP.

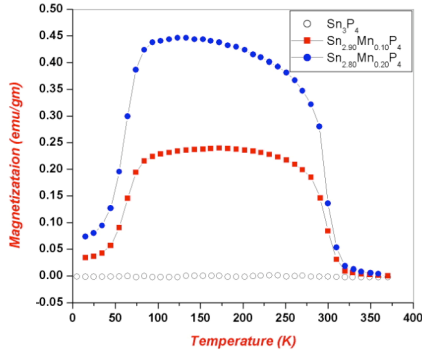


(Fig. 3)

M vs T curves for $\text{Sn}_{3-x}\text{Mn}_x\text{P}_4$

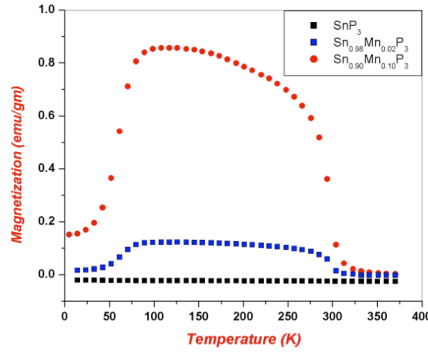


(Fig. 4)

M vs T curves for $\text{Sn}_{1-x}\text{Mn}_x\text{P}_3$

2. Mn doped Zn_3P_2

Binary Zn-P system consists of two stoichiometric congruent melting compounds, namely, Zn_3P_2 and ZnP_2 . The stable polymorph of Zn_3P_2 (tetragonal) and ZnP_2 (monoclinic) are known to be p-type semiconductor with band gap of about 1.4 and 1.2 eV, respectively. These compounds could be prepared by heating elemental Zn and P in an evacuated quartz tube. Series of Mn substituted stoichiometric compositions for Zn_3P_2 , namely $\text{Zn}_{3-x}\text{Mn}_x\text{P}_2$ ($x = 0.03, 0.06, 0.9, 0.15, 0.21$ and 1.00) were prepared from Zn, P and Mn_3P_2 . The phases were characterized by Rietveld refinement of the observed powder x-ray diffraction data (Fig. 5 and 6).

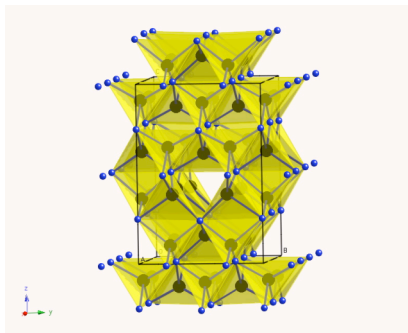


Fig 5.

Crystal structure of Zn_3P_2
(ZnP_4 tetrahedra are shown)

Fig. 6
X-ray diffraction pattern of Zn_3P_2
(Red vertical marks: Si standard)

The variation of unit cell parameters for various compositions shows that only about 2 at % of Zn can be substituted with Mn^{2+} and beyond Mn_2P phase is appeared in the sample. The typical unit cell parameters for the pure Zn_3P_2 and $Zn_{2.97}Mn_{0.03}P_2$ compositions are: $a = 8.1005(1) \text{ \AA}$, $c = 11.4298(3) \text{ \AA}$, $V = 749.99(3) \text{ \AA}^3$; $a = 8.1028(1) \text{ \AA}$, $c = 11.4318(3) \text{ \AA}$, $V = 750.56(3) \text{ \AA}^3$, respectively. The magnetic behaviors of all the compositions were studied in the temperature range of 5 to 370 K (Fig. 7 and 8). These investigations indicate a Curie-Weiss type paramagnetic behavior for Mn substituted Zn_3P_2 dilute systems. An antiferromagnetic interaction between the magnetic ions is concluded from the negative Weiss constants. At higher concentration of Mn the Mn_2P signal ($T_N = 103 \text{ K}$) are observed in magnetic data. The effective magnetic moment for $Zn_{2.97}Mn_{0.03}P_2$ and $Zn_{2.94}Mn_{0.06}P_2$ are about 0.22 and 0.36 per formula unit, indicating that all magnetic ions relatively free and negative Weiss constant (-1 and -8 K, respectively) indicates a possible small antiferromagnetic interactions among the magnetic ions.

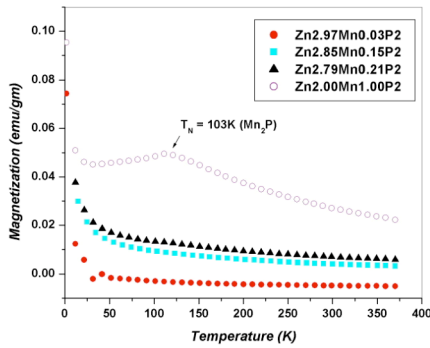


Fig. 7

(M vs T for $Zn_{3-x}Mn_xP_2$ compositions)

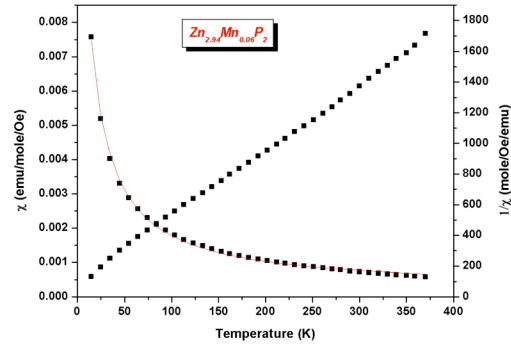


Fig. 8

(χ and $1/\chi$ vs T for $Zn_{2.94}Mn_{0.06}P_2$)

Composition	C	Θ (K)	χ_0 (emu)	μ_{eff} (μ_B)
$Zn_{2.97}Mn_{0.03}P_2$	0.061(1)	-1.14(4)	-0.001	0.22
$Zn_{2.94}Mn_{0.06}P_2$	0.167(3)	-8.1(5)	0.00002	0.36

$$\chi_T \rightarrow \frac{C}{T - \Theta} + \chi_0$$

$$C = \frac{\mu_B^2 N_0 x^2}{3k_B}$$

3. Mn Doped $CaZn_2P_2$ type compounds

Several non magnetic and manganese based AB_2P_2 phosphides exist in $ThCr_2Si_2$ (tetragonal) (Fig 9) and $CaAl_2Si_2$ (hexagonal) (Fig. 10) structure types. Both the structure

types have layered structure with layers of layers of A-cation sandwiched between the B_2P_2 layers. In the $CaAl_2Si_2$ type compounds the B_2P_2 layer is formed with the tetrahedral and inverted tetrahedral arrangement forming corrugated layers of B and P ions.

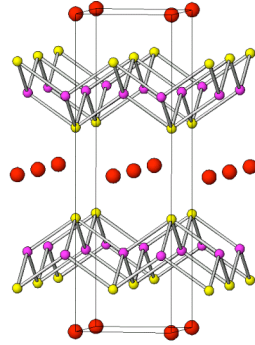


Fig. 9.
Crystal structure of $ThCr_2Si_2$

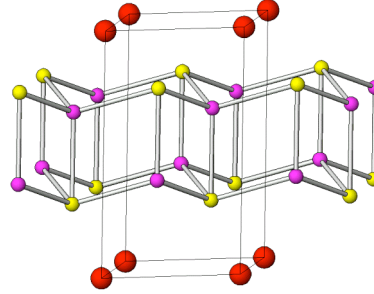


Fig. 10.
Crystal structure of $CaAl_2Si_2$

In the aim of understanding the magnetic properties of the $CaAl_2Si_2$ structure with a very dilute concentration of the magnetic ions a series of $CaZn_{1-x}Mn_xP_2$ compositions have been prepared from stoichiometric amounts of Ca, Zn, P and Mn_3P_2 . On substitution of Mn in $CaZn_2P_2$ the unit cell expands gradually. The typical unit cell parameters for $CaZn_2P_2$ and $CaMn_2P_2$ are: $a = 4.03843(5) \text{ \AA}$, $c = 6.83533(11) \text{ \AA}$ and $a = 4.10230(5) \text{ \AA}$, $c = 6.8565(1) \text{ \AA}$, respectively. The observed unit cell parameters for the mid composition, $CaZnMnP_2$ are: $a = 4.07411(7) \text{ \AA}$, $c = 6.8480(2) \text{ \AA}$. The typical M-P bonds shows a gradual decrease with the Mn substitution indicating the stronger Mn-P bonding nature compared to Zn-P bonds.

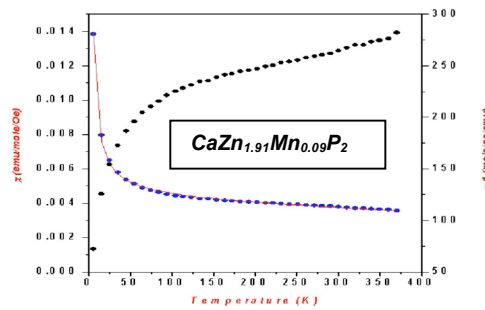


Fig 11.
(χ and $1/\chi$ vs T for $CaZn_{1.91}Mn_{0.09}P_2$)

The temperature dependent magnetizations of various compositions were studied in the temperature range of 370 to 5 K. In all the magnetically diluted compositions Curie-Weiss type paramagnetic behaviors are observed. The variations of magnetic susceptibility with temperature shows a large negative Weiss constant and significantly

lower effective magnetic moments indicating a strong anti-ferromagnetic interaction among the magnetic atoms.

4. *Mn doped Chalcopyrite type ABP₂*

Zinc blende type semiconductors have been attracted for long time due to their important lasing properties. Recent interest on dilute magnetic semiconductor further focused on them for the possible spintronics application. The chalcopyrite type semiconductors are closely related to Zinc blende structure and have been demonstrated as ambient temperature ferromagnetic semiconductor. The crystal structures of zinc blende and chalcopyrite structure are shown in Fig. 12 and 13, which depict their close similarity, besides the metal ion ordering in the later. Mostly, the chalcopyrite type phosphide have intrinsic p-type semiconducting behavior with wide band gap. We have successfully prepared a large number of chalcopyrite host lattice and their Mn substituted derivatives by an optimized heating procedure.

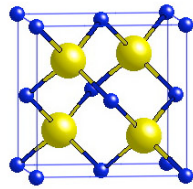


Fig. 12

(Crystal structure of AB zinc blende)

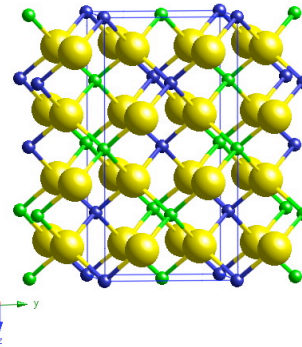


Fig. 13

(Crystal structure of AA'B₂ chalcopyrite)

ABP₂	E_g (eV)	Nature of carrier	Str (Tetra, I-42d), P (u, ¼,1/8) a and c (Å) and u
ZnSiP₂	2.07	p	5.399, 10.436; 0.269
ZnGeP₂	1.99	p	5.465, 10.700; 0.267
ZnSnP₂	1.66	p	5.651, 11.302; 0.239
CdSiP₂	2.05	p	5.680, 10.431; 0.300
CdGeP₂	1.72	p	5.740, 10.775; 0.283
CdSnP₂	1.16	p	5.901, 11.513, 0.265

Typical electrical and structural data for various known chalcopyrite type compounds are given in Table. Typical powder XRD pattern for a representative chalcopyrite compound is shown in Fig 14. The substitutions of Mn in Zn and Cd based chalcopyrite have been carried out.

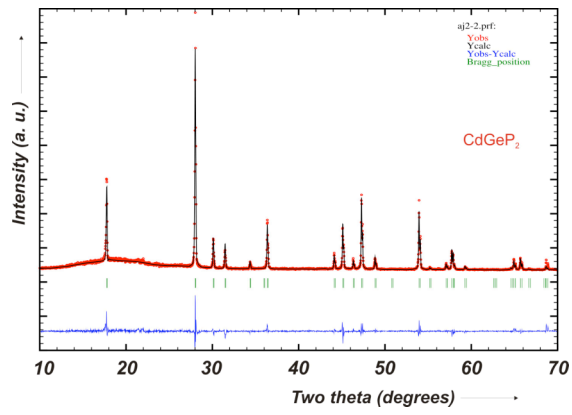


Fig 14

(powder XRD pattern for CdGeP₂)